

High-valence Mo doping for promoted water splitting of Ni layered double hydroxide microcrystals

Kyoungwon Cho, Seungwon Jeong*, Je Hong Park*, Si Beom Yu*, Byeong Jun Kim* and Jeong Ho Ryu*[†]

Center for Research Facilities, Korea National University of Transportation, Chungju 27469, Korea

**Department of Materials Science and Engineering, Korea National University of Transportation, Chungju 27469, Korea*

(Received February 7, 2023)

(Revised April 18, 2023)

(Accepted April 18, 2023)

Abstract The oxygen evolution reaction (OER) is the primary challenge in renewable energy storage technologies, specifically electrochemical water splitting for hydrogen generation. We report effects of Mo doping into Ni layered double hydroxide (Ni-LDH) microcrystal on electrocatalytic activities. In this study, Mo doped Ni-LDH were grown on three-dimensional porous nickel foam (NF) by a facile solvothermal method. Homogeneous LDH structure on the NF was clearly observed. However, the surface microstructure of the nickel foam began to be irregular and collapsed when Mo precursor is doped. Electrocatalytic OER properties were analyzed by Linear sweep voltammetry (LSV) and Electrochemical impedance spectroscopy (EIS). The amount of Mo doping used in the electrocatalytic reaction was found to play a crucial role in improving catalytic activity. The optimum Mo amount introduced into the Ni LDH was discussed with respect to their OER performance.

Key words OER, Ni LDH microcrystals, Mo doping, Water splitting

1. Introduction

The excessive consumption of fossil fuels along with the rapid development of the economy has inevitably caused a severe energy crisis and environmental damage. Water splitting is one of efficient methods to produce clean hydrogen, which can be utilized as an alternative energy for traditional fossil fuels [1,2]. Water electrolysis process contains anodic oxygen evolution reaction (OER) and cathodic hydrogen evolution reaction (HER) [3,4]. The slow kinetic process of OER on the anode always leads to a high overpotential, which would decrease the efficiency of water splitting and result in a slow-going hydrogen production rate on the cathode. Even some noble metal materials such as ruthenium/iridium oxides ($\text{RuO}_2/\text{IrO}_2$) have been proved to be efficient catalysts for OER [5], their large-scale commercialization is limited due to their high cost and low production. Therefore, development of efficient and cheap OER electrocatalysts is extremely necessary for the hydrogen production through water electrolysis [6].

In the past decade, Ni-based catalysts, specially oxides, hydroxides, chalcogenides and others have been applied for OER due to their highly active and low-cost proper-

ties [7]. In order to address the corrosion issue under harsh alkaline environment and increase the reactive areas of Ni-based catalysts [8], the coupling of Ni nanoparticles with carbon materials has become an effective way [9]. Additionally, heteroatom doping in composite catalyst could ulteriorly modify the electron transfer [10]. However, the increased structural complexity would gain difficulty in mechanism analysis for this kind of catalysts. In this case, in-situ techniques along with other effective characterizations becomes strongly needed to better understand the catalytic roles of different parts and mechanism. Here, we synthesized Ni layered double hydroxide (Ni-LDH) microcrystals via facile hydrothermal route on Ni foam (NF).

In this study, we show that high-valence Mo doping into Ni-LDH microcrystals can be a promising strategy for designing highly efficient and commercial electrocatalysts for alkaline OER. Mo was selected as a promising high-valence element for modulating the catalytic properties of Ni-LDH microstructure, where electrical conductivity and number of active sites can be simultaneously enhanced [11]. Benefiting from the optimized electronic structure from the introduced Mo and the conductive NF as the current collector, the Ni-LDH microcrystals on NF displays superior OER performance. Optimum Mo amount introduced into the Ni-LDH microcrystals was discussed on the electrocatalytic OER performance.

[†]Corresponding author
E-mail: jhryu@ut.ac.kr

2. Experimental

2.1. Growth of Mo doped Ni-LDH microcrystals on NF

Nickel foam (NF) was treated with acetone and then with 3 M HCl solution for 10 min using ultrasonication cleaner. The cleaned NF was dried overnight. All the chemicals were purchased from Sigma-Aldrich chemical and were directly used without further purification. For the synthesis of Ni-LDH microcrystal, as-prepared NF was immersed in 25 ml of deionized (DI) water. Then, the resulting solution was transferred to Teflon-lined autoclave and hydrothermally reacted at 160°C for 5 h. The Ni-LDH microcrystals on NF sample was washed several times with DI water. The final Ni-LDH microcrystals grown on NF sample (Ni-LDH/NF) was subsequently dried in vacuum at 80°C for overnight. Synthesis method for Mo doped Ni-LDH on NF samples (χ Mo-Ni-LDH/NF) were same as that of Ni-LDH/NF, except that molybdenum pentachloride (MoCl_5) solution (MoCl_5 0.1 g + H_2O 100 ml) was added before hydrothermal reaction. The added amounts of the MoCl_5 solution were 0.10, 25, 0.50 and 1.00 ml for the $\chi = 0.10, 0.25, 0.50$ and 1.00, respectively.

2.2. Characterizations

Microstructural images of each samples were observed by field emission scanning electron microscopy (FE-SEM; model S4800; Hitachi) equipped with energy dispersive X-ray (EDX). X-ray diffraction (XRD) was performed using a D/MAX-2500/PC (Rigaku) diffractometer at 40 kV and 100 mA with Cu-K α radiation ($\lambda = 0.15418$ nm). The electrochemical properties of catalysts in 1 M KOH were tested using a three-electrode electrochemical cell controlled by an electrochemistry workstation (model Autolab PGSTAT; Metrohm), in which the catalyst grown on NF was used directly as the working electrode [12]. Prior to measurements, the electrolyte (1 M KOH, pH 13.7) was purged for about 10 min with O_2 , and the working electrodes were sealed on all edges with a custom-made acrylate adhesive except for the working surface area of 0.25 cm². Graphite rod and $\text{Hg|Hg}_2\text{SO}_4$ were used as the counter and reference electrodes, respectively. A titration vessel of clear glass was used as a testing cell. The distance between working and reference electrodes was close to 1 cm. Linear sweep voltammetry (LSV) was measured with a scan rate of 0.5 mV/s in a range from 1.20 to 1.8 V vs. a reversible

hydrogen electrode (RHE). Applied potential values were calibrated against RHE, and all polarization curves were iR -corrected. Electrochemical impedance spectroscopy (EIS) measurement was conducted over the frequency range of 0.1~100 kHz at 1.45 V_{RHE} with a sinusoidal amplitude of 5 mV.

3. Results and Discussion

Ni-LDH/NF exhibits poor electrical conductivity, which impedes facile charge transfer between the surface of catalyst and the adsorbed reactant. After Mo doping, electrical properties of χ Mo-Ni-LDH/NF can be significantly improved to easily take up electrons in hydroxyl ions, crucially accelerating water oxidation kinetics. The Mo element can be doped into the transition metal and can stabilize the active β -NiOOH phase in Ni-LDH and facilitate surface intermediate adsorption [11,13].

Typical XRD analysis confirmed the formation of the Ni-LDH/NF and χ Mo-Ni-LDH₂/NF crystal structures as shown in Fig. 1. The strong diffraction peaks near 44° and 51° could be assigned to Ni metal in the NF substrate. The XRD patterns revealed the crystal structure and phase purity of the Ni-LDH/NF microcrystals. Except for the peaks from the NF substrate, all other detectable diffraction peaks at low 2 θ angles could be indexed to the hydrotalcite-like LDH phase. Prominent diffraction peaks for the layered nickel hydroxide were observed from at 19°, 33° and 38°.

Figure 2 shows highly magnified FE-SEM images of the as-grown Ni-LDH/NF and χ Mo-Ni-LDH/NF ($\chi = 0.10, 0.25, 0.50, 1.00$) microcrystals. Figure 2(a) rep-

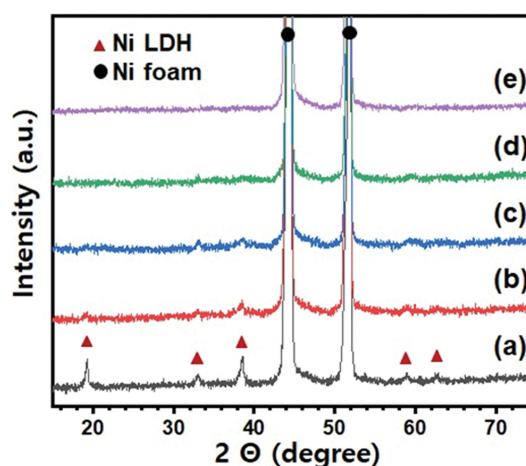


Fig. 1. XRD patterns of the (a) Ni-LDH/NF, (b) 0.01Mo-Ni-LDH/NF, (c) 0.25Mo-Ni-LDH/NF, (d) 0.50Mo-Ni-LDH/NF, and (e) 1.00Mo-Ni-LDH/NF samples.

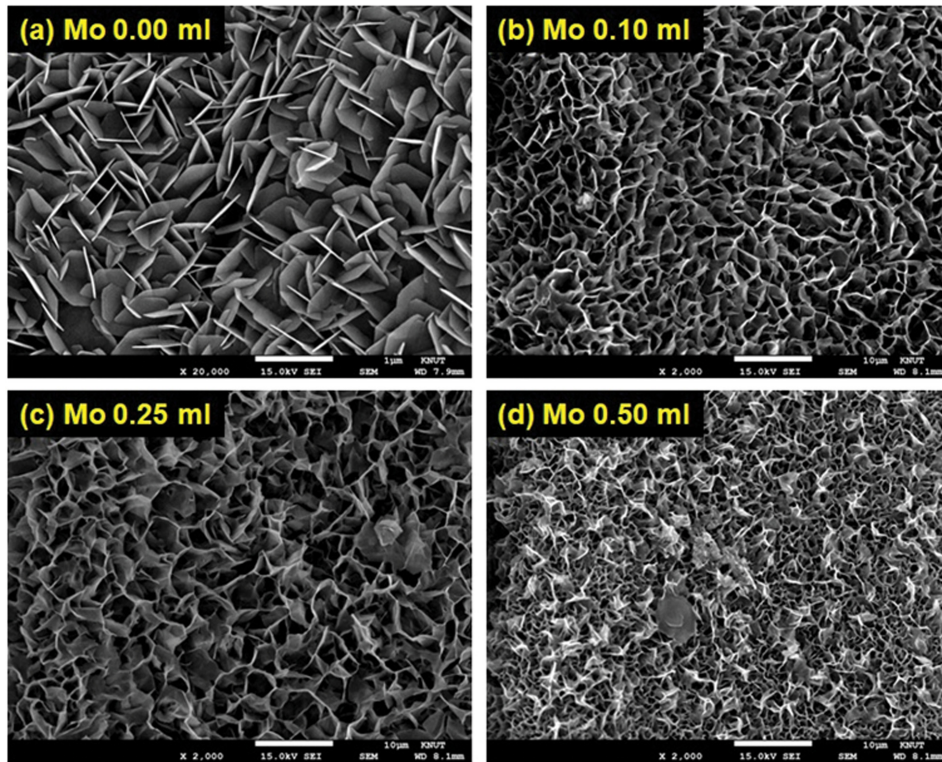


Fig. 2. FE-SEM images for the (a) Ni-LDH/NF, (b) 0.01Mo-Ni-LDH/NF, (c) 0.25Mo-Ni-LDH/NF and (d) 0.50Mo-Ni-LDH/NF samples.

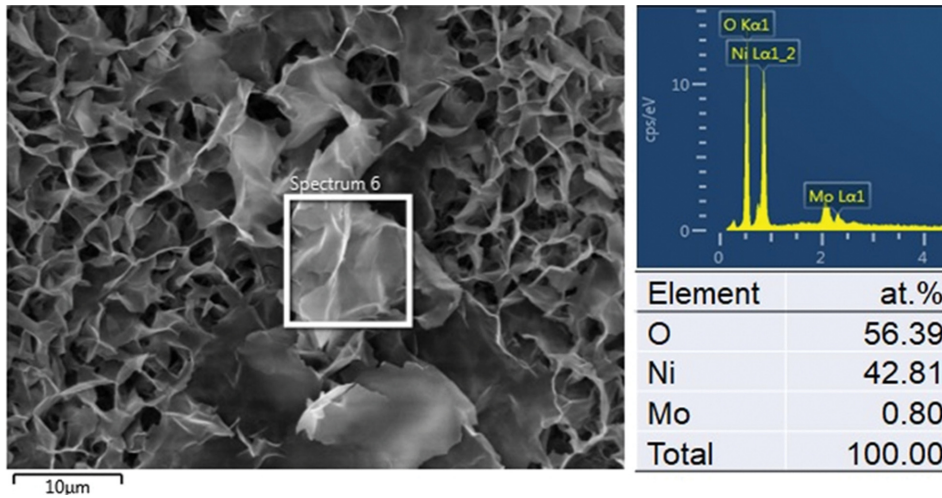


Fig. 3. EDX spectrum and atomic composition of the 0.25Mo-Ni-LDH/NF sample.

resents that large-scale highly interconnected and aligned microplate structure vertically grow on the skeletons of the NF with uniform morphology and dense loading, forming an ordered and 3D network with a highly open and interstitial structure. Homogeneous microplate structure on the 3D macroporous NF was clearly observed for the Ni-LDH/NF and χ Mo-Ni-LDH/NF ($\chi = 0.10, 0.25$) microcrystals. However, when the Mo doping amount (χ) is over 0.50, irregular and collapsed microstructure were found as Fig. 2(d).

Energy-dispersive X-ray (EDX) spectroscopy analysis of the 0.25Mo-Ni-LDH/NF sample revealed the existence of Ni, O and Mo. Figure 3 shows an FE-SEM image, EDX spectrum and atomic composition of the 0.25Mo-Ni-LDH/NF sample. The EDX quantitative data of O, Ni, and Mo elements in 0.25Mo-Ni-LDH/NF indicates all elements are homogeneously distributed. Quantitative EDX analysis showed that the atomic ratio of O:Ni:Mo in the 0.25Mo-Ni-LDH/NF sample was 56.39:42.81:0.80.

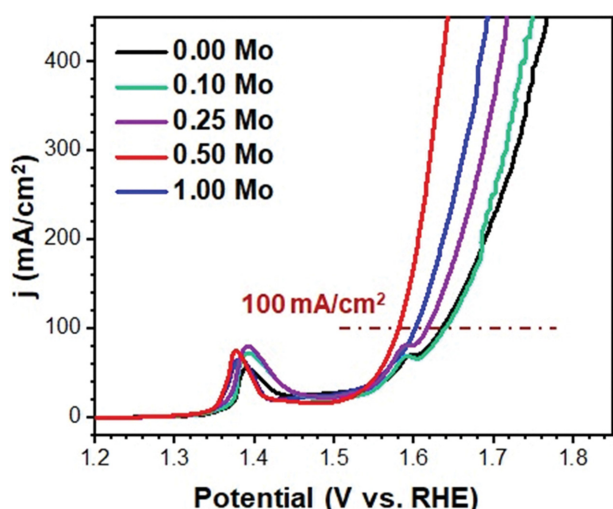


Fig. 4. LSV curves at a scan rate of 0.5 mV/s for electrocatalytic OER properties of the Ni-LDH/NF and χ Mo-Ni-LDH/NF ($\chi = 0.10, 0.25, 0.50, 1.00$) samples.

The electrocatalytic activities of Ni-LDH/NF and χ Mo-Ni-LDH/NF ($\chi = 0.10, 0.25, 0.50, 1.00$) samples were tested in alkaline media (1 M KOH aqueous solution) using a three-electrode system. Linear sweep voltammetry (LSV) was performed at a scan rate of 0.5 mV/s on the samples. NF substrates were directly used as working electrodes, while a rotating disk electrode (RDE) was employed for testing powder samples such as RuO_2 . Notably, χ Mo-Ni-LDH/NF exhibited enhanced catalytic activity for water oxidation compared to Ni-LDH/NF sample. The overpotential (η) required to transmit a current density of 100 mA/cm^2 (η^{100}) is conventionally used as a standard to compare electrocatalytic OER performance [14].

Figure 4 shows LSV curves with a scan rate of 0.5 mV/s for electrocatalytic OER properties of the Ni-LDH/NF and χ Mo-Ni-LDH/NF ($\chi = 0.10, 0.25, 0.50, 1.00$) samples. The η^{100} substantially decreased when Mo was doped into Ni-LDH/NF from $\chi = 0.10$ to 0.50. The 0.50Mo-Ni-LDH/NF sample showed minimum η^{100} of 320 mV, which can be beneficial for practical electrolysis applications. The amount of Mo incorporation used in the reaction was found to play a crucial role in improving catalytic activity. In terms of overpotential, the Mo content in 0.50Mo-Ni-LDH₂/NF resulted in the best catalytic activity for water oxidation. However, further increasing Mo content to 1.00Mo-Ni-LDH/NF significantly disturbed its catalytic activity, which may be related to irregular and collapsed microstructure grown on the nickel foam substrate as shown in Fig. 2(d).

Tafel plots of the samples were derived from the measured LSV curves based on the Tafel equation ($\eta = b \times$

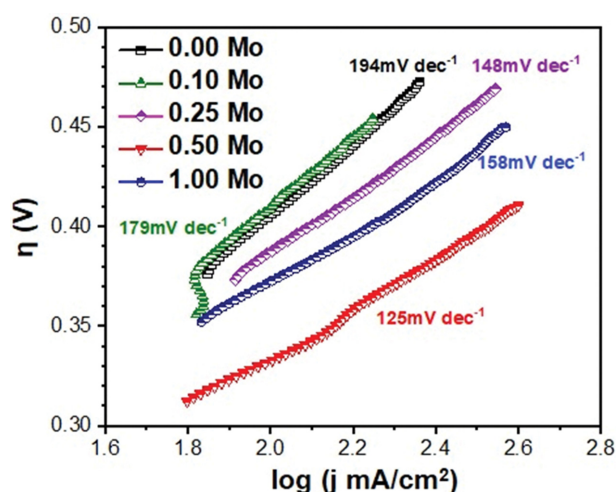


Fig. 5. Tafel slopes of Ni-LDH/NF and χ Mo-Ni-LDH/NF ($\chi = 0.10, 0.25, 0.50, 1.00$) samples derived from the measured LSV curves.

$\log j + a$), where η is the overpotential, j is the current density, and b is the Tafel slope. Tafel slopes of Ni-LDH/NF and χ Mo-Ni-LDH/NF were calculated and represented in Fig. 5. The measured Tafel slopes of the Ni-LDH/NF was 194 mV/dec, and the χ Mo-Ni-LDH/NF were 179, 148, 125 and 158 mV/dec for the χ values of 0.1, 0.25, 0.50 and 1.00, respectively. Among the samples, 0.50Mo-Ni-LDH/NF exhibited the smallest Tafel slope (125 mV/dec) compared to Ni-LDH/NF (194 mV/dec), highlighting the potential use of Mo-Ni-LDH/NF for industrial electrolyzer because a smaller Tafel slope is desirable to reduce power losses [15].

4. Summary

The Ni-LDH and χ Mo-Ni-LDH ($\chi = 0.1, 0.25, 0.50$ and 1.00) microcrystals were successfully grown on nickel foam (NF) via hydrothermal reaction at 160°C for 5 h as highly efficient and low-cost electrocatalysts for water oxidation under alkaline conditions. Homogeneous nanoplate structure on the NF was clearly observed for the Ni-LDH and χ Mo-Ni-LDH samples. When Mo doping amount (χ) is higher over 0.50, irregular and collapsed nanostructures were found on the surface of NF. The electrocatalyst of 0.50Mo-Ni-LDH/NF sample provided current densities of 100 mA/cm^2 at overpotentials of 320 mV, respectively, with a Tafel slope of 125 mV/dec in an alkaline medium. These results demonstrate that the χ Mo-Ni-LDH/NF are promising electrocatalysts for water oxidation and optimum Mo doping content (χ) is 0.5.

Acknowledgement

This work was supported by the National Research Foundation of Korea (NRF) grant funded by the Korea government (MSIT) (No. 2022R1A2C2010162).

References

- [1] B. You and Y. Sun, "Innovative strategies for electrocatalytic water splitting", *Acc. Chem. Res.* 51 (2018) 1571.
- [2] Y. Shi and B. Zhang, "Recent advances in transition metal phosphide nanomaterials: synthesis and applications in hydrogen evolution reaction", *Chem. Soc. Rev.* 45 (2016) 1529.
- [3] M. Zeng and Y. Li, "Recent advances in heterogeneous electrocatalysts for the hydrogen evolution reaction", *J. Mater. Chem. A* 3 (2015) 14942.
- [4] H.J. Lee, K. Cho and J.H. Ryu, *J. Korean Cryst. Growth Cryst. Technol.* 30 (2020) 17.
- [5] W. Zhang, W. Wang, H. Shi, Y. Liang, J. Fu and M. Zhu, "Surface plasmon-driven photoelectrochemical water splitting of aligned ZnO nanorod arrays decorated with loading-controllable Au nanoparticles", *Sol. Energy Mater. Sol. Cells* 180 (2018) 25.
- [6] R. Kant, S. Pathak and V. Dutta, "Design and fabrication of sandwich-structured α -Fe₂O₃/Au/ZnO photoanode for photoelectrochemical water splitting", *Sol. Energy Mater. Sol. Cells* 178 (2018) 38.
- [7] S.A. Shah, Z. Ji, X. Shen, X. Yue, G. Zhu, K. Xu, A. Yuan, N. Ullah, J. Zhu, P. Song and X. Li, "Thermal synthesis of FeNi@nitrogen-doped graphene dispersed on nitrogendoped carbon matrix as an excellent electrocatalyst for oxygen evolution reaction", *ACS Appl. Energy Mater.* 2 (2019) 4075.
- [8] T. Zhang, M.-Y. Wu, D.-Y. Yan, J. Mao, H. Liu, W.-B. Hu, X.-W. Du, T. Ling and S.-Z. Qiao, "Engineering oxygen vacancy on NiO nanorod arrays for alkaline hydrogen evolution", *Nano Energy* 43 (2018) 103.
- [9] L. Lin, T. Liu, B. Miao and W. Zeng, "Hydrothermal fabrication of uniform hexagonal NiO nanosheet: Structure, growth and response", *Mater. Lett.* 102-103 (2013) 43.
- [10] G-Q. Han, Y.-R. Liu, W.-H. Hu, B. Dong, X. Li, X. Shang, Y.-M. Chai, Y.-Q. Liu and C.-G. Liu, "Three dimensional nickel oxides/nickel structure by in situ electro-oxidation of nickel foam as robust electrocatalyst for oxygen evolution reaction", *Appl. Surf. Sci.* 359 (2015) 172.
- [11] L. Wei, M. Du, R. Zhao, F. Lv, L. Li, L. Zhang, D. Zhou and J. Su, "High-valence Mo doping for highly promoted water oxidation of NiFe (oxy)hydroxide", *J. Mater. Chem. A* 10 (2022) 23790.
- [12] M. Xu and M. Wei, "Layered double hydroxide-based catalysts: Recent advances in preparation, structure, and applications", *Adv. Funct. Mater.* 28 (2018) 1802943.
- [13] J. Masa, I. Sinev, H. Mistry, E. Ventosa, M. de la Mata, J. Arbiol, M. Muhler, B. Roldan Cuenya and W. Schuhmann, "Ultrathin high surface area nickel boride (Ni₃B) nanosheets as highly efficient electrocatalyst for oxygen evolution", *Adv. Energy Mater.* 7 (2017) 1700381.
- [14] C.C.L. McCrory, S. Jung, J.C. Peters and T.F. Jaramillo, "Benchmarking heterogeneous electrocatalysts for the oxygen evolution reaction", *J. Am. Chem. Soc.* 135 (2013) 16977.
- [15] N.T. Suen, S.F. Hung, Q. Quan, N. Zhang, Y.J. Xu and H.M. Chen, "Electrocatalysis for the oxygen evolution reaction: Recent development and future perspectives", *Chem. Soc. Rev.* 46 (2017) 337.